

## ARTICLE

## Water-Polyamide Chemical Interplay in Desalination Membranes explored by Ambient Pressure X-ray Photoelectron Spectroscopy

Received 00th January 20xx,  
Accepted 00th January 20xx

DOI: 10.1039/x0xx00000x

Sabrina M. Gericke,<sup>a,#</sup> William D. Mulhearn,<sup>c</sup> Dana E. Goodacre,<sup>b,d</sup> Joseph Raso,<sup>a,\*</sup> Daniel J. Miller,<sup>a</sup> Lauryn Carver,<sup>a</sup> Slavomír Nemšák,<sup>b</sup> Osman Karslıoğlu,<sup>a,&</sup> Lena Trotochaud,<sup>a,§</sup> Hendrik Bluhm,<sup>a,b,&</sup> Christopher M. Stafford,<sup>c</sup> Christin Buechner<sup>a</sup>

Reverse osmosis using aromatic polyamide membranes is currently the most important technology for seawater desalination. The performance of reverse osmosis membranes is highly dependent on the interplay of their surface chemical groups with water and water contaminants. In order to better understand the underlying mechanisms of these membranes, we study ultrathin polyamide films that chemically resemble reverse osmosis membranes, using ambient pressure X-ray photoelectron spectroscopy. This technique can identify the functional groups at the membrane-water interface and allows monitoring of small shifts in the electron binding energy that indicate interaction with water. We observe deprotonation of free acid groups and formation of a 'water complex' with nitrogen groups in the polymer upon exposure of the membrane to water vapour. The chemical changes are reversed when water is removed from the membrane. While the correlation between functional groups and water uptake is an established one, this experiment serves to understand the nature of their chemical interaction, and opens up possibilities for tailoring future materials to specific requirements.

### Introduction

In the context of global economic growth, the need for potable water as well as highly deionized water for technological applications is steadily increasing.<sup>1</sup> Coupled with increasingly unreliable precipitation patterns, water purification is a keystone technology for many regions of the world. The predominant method for purifying saltwater in particular, reverse osmosis (RO) desalination, relies on a composite membrane with an active layer of cross-linked, aromatic polyamide (PA) which allows water to permeate.<sup>2</sup> A saltwater feed is pressurized against this membrane, and water dissolves into the polymer, subsequently migrating through the material while NaCl is rejected at rates of 99 % or more.<sup>3</sup> Other common water contaminants are rejected with lower efficiencies, with some broad correlations observed based on the charge state of the ion.<sup>3</sup> Fundamental studies of the membrane surface chemistry are needed to understand the nature of the strong variation in rejection rates, which often necessitates additional

pretreatment of feedwater streams, multiple passes or a combination of different purification steps, depending on the water source. A more detailed view of the surface chemistry can also enhance the understanding of surface fouling, i.e. the unwanted accumulation of matter (mineral scaling or biofilm) on the membrane surface, leading to drastic increases in membrane resistance over time. Surface fouling eventually requires module replacement, contributing significantly to operation and maintenance costs in RO desalination.<sup>4,5</sup> Solving these challenges requires a detailed look at the surface chemical groups of the membrane and their interaction with the components of a feed water stream. Ambient pressure X-ray photoelectron spectroscopy (APXPS) can provide this information with high chemical fidelity, resolving different chemical groups and binding energy shifts depending on the chemical environment, e.g. the presence of aqueous solutions in contact with the membrane.<sup>6</sup> A simple thin film preparation routine for aromatic, cross-linked polyamide films was recently published by Stafford et al.,<sup>7</sup> providing reproducible model systems that replicate the chemistry of commercial RO desalination membranes.<sup>8</sup>

In this paper, we investigate the interplay of the surface chemical groups of thin film model polyamide membranes with water vapour. We observe a strong interaction of the free acid groups, amine groups and amide groups in contact with water, evidenced by a clear chemical shift that is reversible. When characterizing soft matter with ultrabright X-ray light, the stability under the beam is always a concern as well. We characterize the behaviour of the polymer under the X-ray beam and discuss mitigation strategies for reducing the

<sup>a</sup>Chemical Sciences Division and <sup>b</sup>Advanced Light Source, Lawrence Berkeley National Laboratory, Berkeley, CA 94720, USA

<sup>c</sup>Materials Science and Engineering Division, National Institute of Standards and Technology, Gaithersburg, MD 20899, USA

<sup>d</sup>Chemical Sciences, The University of Auckland, Auckland 1010, NZ

<sup>\*</sup>Present address: Department of Physics, Lund University, 221 00 Lund, SE

<sup>&</sup>Present address: Department of Chemistry, University of Colorado, Boulder, CO 80304, USA

<sup>§</sup>Present address: Department of Inorganic Chemistry, Fritz-Haber-Institute of the Max-Planck-Society, D-14195 Berlin, DE

<sup>§</sup>Present address: Center for Water, Sanitation, Hygiene, and Infectious Disease, Duke University, Durham, NC 27708, USA

Electronic Supplementary Information (ESI) available: See DOI: 10.1039/x0xx00000x

damaging effects of X-ray exposure on the polyamide membranes.

## Experimental

Thin films of aromatic polyamide were prepared via molecular layer-by-layer spin coating, as described in the literature.<sup>7,9</sup> Trimesoyl chloride or terephthaloyl chloride (monomers A3 and A2) and *m*-phenylene diamine (monomer B2) were sequentially deposited on wafer substrates, coated with Au or Pt (see supplement for molecular structures). Either one of the monomers can be deposited first and can terminate the deposition. One deposition cycle of monomer A and B is designated as one monolayer (ML) and contributes between 0.33 nm and 1 nm to the film thickness.<sup>7,10,11</sup> Molecular layer-by-layer produced polyamide films have been reported to exhibit largely similar zeta potential values and contact angles as polyamide films produced by interfacial polymerization.<sup>10,12</sup> See the supplement for more details on the preparation. For the results presented in this manuscript, seven samples with PA films between 1 ML and 20 ML were investigated, as well as reference measurements on pure layers of monomer A or B, respectively. The spectra and chemical interactions discussed in the following section are representative for the range of samples, with quantitative differences based on sample thickness, monomer termination and relative humidity (RH) setting of each respective experiment.

The characterization of such films in ultrahigh vacuum (UHV) was previously reported and showed the presence of benzyl rings, amide groups, as well as unpolymerized acid groups and amine groups.<sup>8</sup> It was also shown that under UHV, X-ray beam damage to the polymer is not significant.

Ambient pressure XPS data were recorded using two synchrotron-based APXPS endstations utilizing soft X-rays for core-level spectroscopy, namely APXPS-1 [Ref. <sup>13</sup>] at BL 11.0.2 and the APXPS endstation at BL 9.3.2 [Ref. <sup>14</sup>] of the Advanced Light Source. The ex-situ prepared samples were introduced to the measurement chambers after storing between 1 week and 14 months under ambient conditions. For characterizing 'dry' films, the samples were heated in the experiment chamber to between 50 °C and 80 °C until degassing ceased, usually between 30 min and 60 min. For studying the interaction with water, a flask of highly demineralized (MilliPore, 18 MΩ·cm) water was mounted to the chamber with a leak valve. The water was degassed using at least three freeze-pump-thaw cycles. While dosing water in the range from 10<sup>-6</sup> Torr to about 2 Torr,<sup>15</sup> the sample was cooled using an isopropanol chiller to temperatures down to 275 K, achieving relative humidity up to 20 % at the lowest temperature and highest water vapour pressure.

C 1s, O 1s, N 1s, and Au 4f core levels were taken at incident photon energies of 490 eV, 735 eV, 600 eV and 290 eV, respectively, i.e. with 200 eV photoelectron kinetic energy, to ensure comparable surface sensitivity. The binding energy axis in the O 1s, N 1s and C 1s spectra was calibrated to the low binding energy (BE) peak of the C 1s spectrum, which consists

mainly of benzyl carbons with a BE of 284.7 eV.<sup>16</sup> To that end, C 1s spectra were also measured at the same photon energy as for O 1s, N 1s and Au 4f. Spectra were fitted with the KolXPDS software package.<sup>17</sup> For Au 4f and C 1s spectra, a Shirley background was subtracted. For O 1s and N 1s spectra, a linear background was subtracted. Au 4f spectra were fitted with convolution of Doniach-Sunjić and Gaussian peak shapes, while C 1s, O 1s and N 1s spectra were fitted with Voigt peak shapes.

## Results and discussion

In the following, we discuss the changes in each core level spectrum that were observed upon dosing of water vapour into the chamber. By taking spectra of each sample position in a dry state before water dosing, while water is present, and after water dosing, one can identify clear changes in the peak areas of certain functional groups which can be used to infer their interactions with water. The qualitative changes that are assigned to the interaction between the polyamide film and water are reproducibly observed over a range of samples (see supplement for details on the various samples). The magnitude of the observed changes in peak areas correlates with the relative humidity set in each experiment, as well as with the prevalence of specific chemical moieties, which can vary depending on the film preparation process.

The O 1s spectrum taken at the start of the experiment under dry conditions (bottom trace in Figure 1) exhibits two peaks, which have been discussed previously.<sup>8</sup> The low BE peak at 531.3 eV is consistent with literature values for carbonyl oxygen groups<sup>16,18,19</sup> and is assigned to the amide groups in the polyamide sample. The other peak at 532.7 eV contains contributions from a variety of chemical species. Based on BEs from literature, as well as the behaviour of this peak during

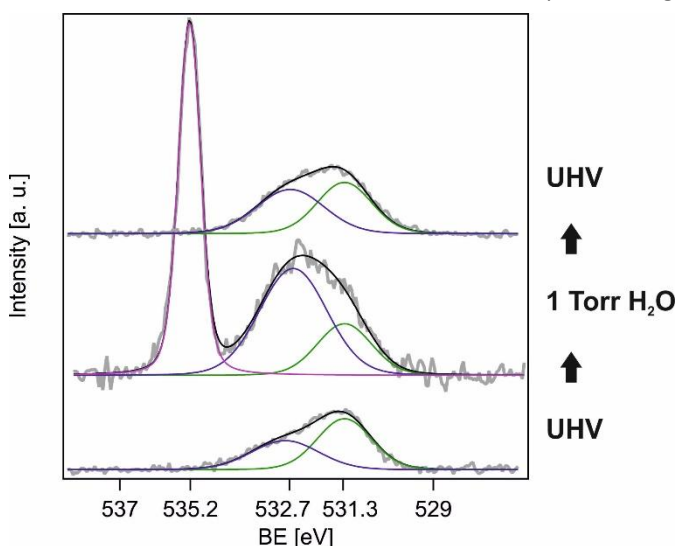


Figure 1: Changes in the O1s spectrum when a 1.5 ML film (ABA) is exposed to 20.5 % RH. Data are shown in grey and the fit envelope in black, with peaks assigned to C=O groups (green), a convolution of OH groups from the polymer and adventitious origin, and water (dark blue), and gas phase water (pink). The BE of water overlaps with species in the sample.

heating and irradiation, it was concluded it contains COOH

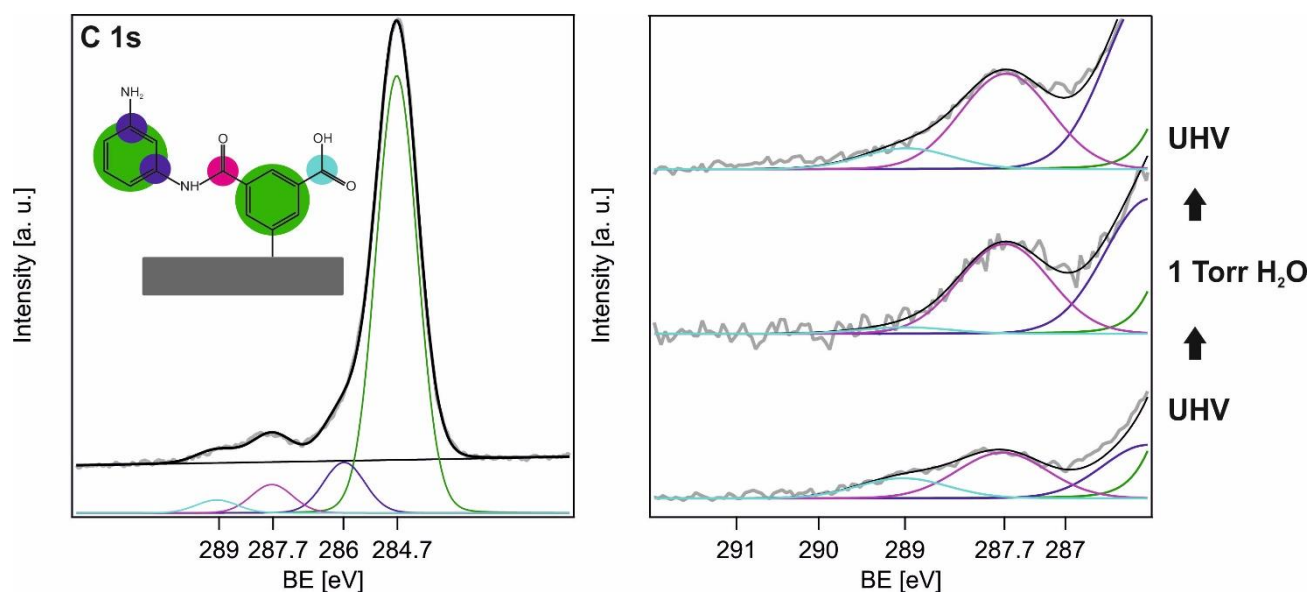


Figure 2: Changes in the C 1s spectrum when a 1.5 ML film (ABA) is exposed to 20.5 % RH. Left: Entire C1s region at UHV, data in grey and fit in black, with peaks assigned to C-C groups (green), C-N groups (dark blue), C=O groups (pink) and COOH groups (cyan). A schematic of the polymer repeat unit shows the different carbon species in the same color coding. Right: The high BE region is shown for successive measurements at UHV, 1 Torr water pressure and UHV again. The COOH region decreases in intensity when water is present and recovers when the film is dried again.

groups, residual water, and potentially adventitious carbon-hydroxyl species.<sup>8</sup> This peak grows considerably when water vapour is dosed into the vacuum chamber (middle trace in Fig. 1), indicating the adsorption of water onto the membrane.<sup>13</sup> Since this peak comprises multiple chemical species with potentially slightly different BEs, and only one of them likely causes the change in peak area, it is possible that the effective peak position slightly shifts as a result. This effect, however, appears to be smaller than the experimental resolution, which was around 0.35 eV for this experiment. In addition, a very sharp peak at 535.2 eV is observed, which is typical for gas phase water molecules.<sup>13</sup> When the water vapour is pumped out of the chamber and the sample is heated again to at least 50 °C in order to drive out the remaining adsorbed water (see top spectrum in Fig. 1), the gas phase water peak disappears, and the peak at 532.7 eV is reduced in size. Even after an extended period of vacuum recovery ( $\approx 10$  hrs) and heating the sample, the peak area does not fully recover its initial size, indicating some irreversible change, which we discuss later.

Figure 2 shows the evolution of the C 1s region during the same experiment. On the left side, the full spectrum as observed in UHV is shown, with a schematic of the polymer repeat unit in colour coding corresponding to the fitted peak components. The peak positions found for aromatic C-C groups (284.7 eV), C-N groups (286 eV), C=O groups (287.7 eV) and COOH groups (289 eV) are consistent with literature values.<sup>8</sup> The right panel in Figure 2 shows an enlargement of the high BE region of the C 1s spectrum before, during and after water exposure. In the presence of water, the COOH peak disappears, and the C=O peak increases in intensity compared to the initial spectrum taken under vacuum conditions. While the data in Figure 2 were taken at the maximum RH of 20.5 %, the onset of this effect is visible already at 2 % RH. This behaviour is consistent with a

deprotonation of the COOH group to a COO<sup>-</sup> group, which has been observed to happen readily at pH = 7 or less.<sup>6,20–22</sup> The resultant COO<sup>-</sup> group has a similar BE as the amide-C=O group, and therefore contributes to the pink peak that is fitted at 287.7 eV. When the water is removed from the sample, the peak at 289 eV reappears, indicating the re-protonation of the COOH group. It should be noted that the peak area of the C=O peak does not diminish correspondingly, which can again be assigned to irreversible changes that will be discussed later.

The changes in the N 1s spectrum are shown in Figure 3. Initially, the N 1s signal is mainly composed of two chemically different nitrogen species. The main peak position at 399.7 eV is consistent with nitrogen in amide groups.<sup>8</sup> A signal at lower BE (398.6 eV) is assigned to amines that occur as chain termination groups. A very small shoulder at higher BE can sometimes be observed as well; when water is dosed, this signal around 401.8 eV increases in area. The onset of this increase can be observed at relative humidities of as little as 1 % (the highest RH shown in Figure 3 is 9 %). Also visible in Figure 3 is a sharp peak around 405 eV, originating from N<sub>2</sub> gas which leaked into the chamber through a badly sealed vacuum fitting. We observe the same qualitative changes in all samples, regardless of the presence of N<sub>2</sub> gas in the chamber.

We can assume the newly formed N 1s peak at 401.8 eV to be a species in which water interacts with nitrogen containing groups, pulling electron density from the nitrogen free electron pairs and thus causing a shift to higher binding energy. This interaction could theoretically happen with either the existing amine groups, the amide groups, or both. The areas of all three peaks change during the experiment, indicating that the amide and the amine species both undergo an interaction with water. The area of the amine peak decreases from 30 % of the initial overall peak area to 8 %, while the high-BE peak increases from

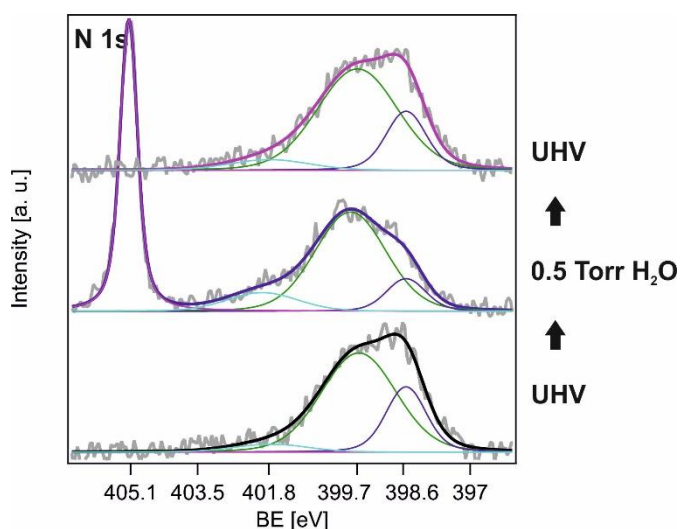


Figure 3: Changes in the N 1s spectrum when a 2.5 ML film (BABAB) is exposed to 9 % RH. Data are shown in grey and the fit envelope in black, with peaks assigned to amide groups (green), amine groups (dark blue), N<sub>2</sub> gas (pink) and amide-water complex species (cyan). When exposed to water vapour, the peak assigned to a water complex formed with the amide groups in the film increases in area.

5 % to 15 % and the middle peak exhibits a slight increase. Reference measurements (see supplement) of a monolayer of the mPD monomer on Au substrates (hence containing amine groups, but no amide groups), show a  $\approx 1$  eV shift to higher BE when amine interacts with water. We conclude that amine species undergoing such an interaction in the polyamide sample shown here, would exhibit a chemical shift of their peak position, rendering it indistinguishable from the amide peak at 399.7 eV BE.

We can therefore assign the formation of the new peak at  $\approx 401.8$  eV to water interaction with the amide group. The observed chemical shift with respect to the central peak position is in agreement with the formation of an ammonium-type complex with water as predicted by DFT.<sup>23</sup> In this chemical environment, a water molecule is located near the amide group, with the water's hydrogen atom oriented towards the amide group. A true protonation of the amide or amine group would be expected to cause chemical shifts of 3 eV or larger,<sup>6,23</sup> but the smaller shift we observe of roughly 2 eV is consistent with the water molecule not fully transferring its proton to the amide. This hypothesis is further corroborated by the reversibility of the change upon water evacuation (top trace in Fig. 3), indicating that water molecules are involved in the formation of the complex that gives rise to the peak at 401.8 eV BE.

These direct observations of the chemical interaction of the polymer constituents with water can be correlated with other reports on the effects of exposing polyamide to water. Using infrared methods, correlations of polymer composition in aromatic polyamides and water uptake ability have been observed, indicating the important role that amide, carboxylic acid, and amine groups play in the water interaction.<sup>24,25</sup> Furthermore, infrared studies of water uptake on nylon 6,6 samples reported shifts in vibrational frequencies assigned to

bonds involved in the amide group.<sup>26</sup> These and other observations indicate that water molecules weaken existing hydrogen bonds inherent to the polymer network by forming new hydrogen bonds with the carbonyl groups and the N-H groups.<sup>25–27</sup> The data presented here were obtained at low relative humidities, and hence likely represent the initial onset of the interaction between water and polymer.

Molecular dynamics simulations of RO membranes found that water flow around carboxyl or amino groups is slower than around the benzene rings.<sup>28</sup> The chemical shifts we observe are reversed when water is removed, indicating that water molecules need to be present to induce the deprotonation in the case of COOH, and complexation in the case of amide and amine, respectively. These specific interactions might cause water molecules to slow down while migrating through the membrane to the permeate, low pressure side, in line with the molecular dynamics simulations. At the same time, it is possible that a strong interaction facilitates the initial entrance of water molecules into the active layer, which is a prerequisite to subsequent diffusion. This function of the polar groups in facilitating transport would be reminiscent of water transport through aquaporin channels found in living organisms, which have been shown to facilitate water transport with high selectivity via hydrogen bonding of carboxyl- and amine-groups along the walls of the channel.<sup>29</sup>

While the specific interactions between the polymer and water observed here appear reversible, we also observe changes in the spectra that remain after the polymer is dried. These irreversible changes are different from the beam-induced changes that we reported on previously.<sup>8</sup> When polyamides were investigated in UHV, the aromatic backbone proved relatively robust against beam damage, which is in line with previous literature studies.<sup>8</sup> The presence of water fundamentally changes the amount of X-ray beam damage that is observed in the spectra.

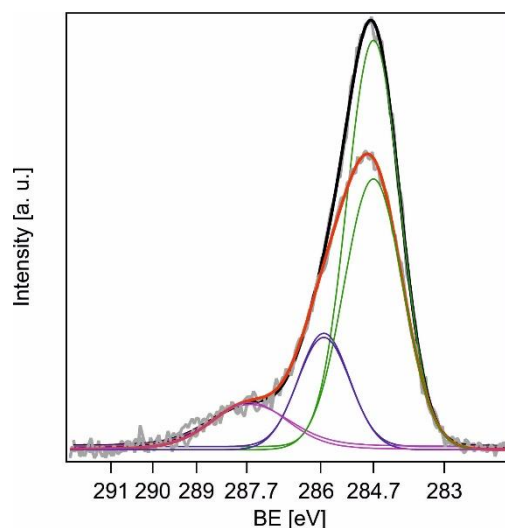


Figure 4: Beam-induced changes to a 1 ML (AB) polyamide film in the presence of water. Black trace before exposure, red trace after exposure to 100 mTorr H<sub>2</sub>O and X-rays for 75 min.

Beam damage can be characterized by comparing spectra taken on the same sample position over a period of time. Common beam damage features are changes in the relative intensity of peaks, indicating a chemical transformation of a certain chemical species, or overall loss of intensity in a core level spectrum, indicating net mass loss of a certain element during exposure to X-rays.

Figure 4 shows the first and last spectrum in a series of C 1s spectra that were taken at 735 eV excitation energy on a polyamide film in the presence of 100 mTorr water, over the course of 75 min. The photon flux was calibrated to be  $1.3 \times 10^7$  photons  $s^{-1} \mu m^{-2}$ . We observe an overall decrease in the C 1s intensity of 20 %, focused entirely on the peak assigned to the benzyl groups. This pattern indicates significant damage to the benzyl rings occurring during the measurement, which is qualitatively different from observations under UHV conditions.<sup>8</sup> The most straightforward explanation for the characteristic change in beam damage is that the ionizing radiation interacts with water molecules present in the experiment chamber in the vapour phase, creating highly reactive species, such as OH· radicals, which have been observed at synchrotron experiments in significant concentrations.<sup>30–32</sup> Furthermore, H<sub>2</sub>O<sub>2</sub> molecules have been observed to form spontaneously in ppm concentrations upon nebulization of water into microdroplets.<sup>33</sup> The OH· radicals readily react with conjugated double bonds which are found in the polyamide molecules.<sup>34–36</sup>

In the corresponding O 1s spectra, we observe little change with X-ray exposure, except for a slight, but consistent mass gain in the high-BE peak, assigned to OH groups in the polymer and in adventitious carbon contaminations, as well as in adsorbed water. This increase of approximately 5 % of the initial peak area remains after the sample is dried again, suggesting the creation of new OH groups during the exposure. The N 1s spectrum shows no consistent change, while the Au 4f spectrum reflects the mass loss in the polymer film, showing an increase in overall intensity.

In the case of samples irradiated at higher relative humidities, such as for the datasets presented in Figures 1–3, the effects of irradiation on the sample are qualitatively similar. At higher water vapour pressures, the formation of OH groups on the surface observed in the O 1s spectrum becomes more pronounced. The same effect then also leads to an increase in the high-BE peaks (blue and pink) of the C 1s spectrum.

These changes are observed both under the beam spot as well as on adjacent sample positions that were not directly exposed to photons. This result also indicates the formation of radicals in the water vapour that subsequently react with the sample surface. Radical species are formed under the beam but can diffuse and travel to sample positions that were not irradiated. Based on our observations, it is possible to obtain data from a pristine sample by periodically moving to new sample positions, but the step size should be at least two times the step size used under UHV conditions. Since the appropriate step size depends on the mean free path of the reactive species and hence the

specific experimental conditions, a careful calibration for each experiment is advisable.

## Conclusions

APXPS investigations of the fundamental, chemical interplay between polyamide films and water molecules were undertaken at relative humidities of up to 20 %. The data show the disappearance of a peak with a BE of 289 eV in the C 1s spectra upon adding water, which is consistent with the deprotonation of COOH groups. The data also show the formation of a water-nitrogen complex at the amide groups and amine groups. These species most likely determine how water molecules can pass through polyamide membrane materials, and are thus crucial for the application of these materials in desalination membranes. The extent of radiation damage occurring over the course of the measurement has also been described, providing a solid basis for further investigations. Going forward, this approach can help to shine light on the highly specific and selective interaction of polyamide desalination systems with various water contaminants.

## Conflicts of interest

There are no conflicts to declare.

## Acknowledgements

This work, including resources of the Advanced Light Source, a DOE Office of Science User Facility, the MES beamline 11.0.2, and beamline 9.3.2, was supported by the Director, Office of Science, Office of Basic Energy Sciences, Division of Chemical Sciences, Geosciences, and Biosciences of the US Department of Energy under Contract No. DE-AC02-05CH11231. C.B. is grateful for support from the Alexander von Humboldt Foundation through a Feodor Lynen Research Fellowship. S.G. is grateful for support from a PROMOS scholarship provided by the Freie Universität Berlin. D.E.G. is grateful for an ALS Doctoral Fellowship in Residence. This work was supported in part by the U.S. Department of Energy, Office of Science, Office of Workforce Development for Teachers and Scientists (WDTs) under the Science Undergraduate Laboratory Internship (SULI) program.

## Notes and references

- 1 C. A. Schlosser, K. Strzepak, X. Gao, C. Fant, É. Blanc, S. Paltsev, H. Jacoby, J. Reilly and A. Gueneau, *Earth's Futur.*, 2014, **2**, 341–361.
- 2 K. P. Lee, T. C. Arnot and D. Mattia, *J. Memb. Sci.*, 2011, **370**, 1–22.
- 3 G. M. Geise, H.-S. Lee, D. J. Miller, B. D. Freeman, J. E. McGrath and D. R. Paul, *J. Polym. Sci. Part B Polym. Phys.*, 2010, **48**, 1685–1718.
- 4 WaterReuse Association, *Seawater Desalination Costs*,

- 2012.
- 5 N. M. Farhat, C. Christodoulou, P. Placotas, B. Blankert, O. Sallangos and J. S. Vrouwenvelder, *Desalination*, 2020, **473**, 114172.
- 6 B. Xu, M. I. Jacobs, O. Kostko and M. Ahmed, *ChemPhysChem*, 2017, **18**, 1503–1506.
- 7 P. M. Johnson, J. Yoon, J. Y. Kelly, J. A. Howarter and C. M. Stafford, *J. Polym. Sci. Part B Polym. Phys.*, 2012, **50**, 168–173.
- 8 C. Buechner, S. M. Gericke, L. Trotochaud, O. Karslioglu, J. Raso and H. Bluhm, *Langmuir*, 2019, **35**, 11315–11321.
- 9 E. P. Chan, J.-H. H. Lee, J. Y. Chung and C. M. Stafford, *Rev. Sci. Instrum.*, 2012, **83**, 114102.
- 10 J.-E. Gu, S. Lee, C. M. Stafford, J. S. Lee, W. Choi, B.-Y. Kim, K.-Y. Baek, E. P. Chan, J. Y. Chung, J. Bang and J.-H. Lee, *Adv. Mater.*, 2013, **25**, 4778–4782.
- 11 E. P. Chan, A. P. Young, J.-H. H. Lee and C. M. Stafford, *J. Polym. Sci. Part B Polym. Phys.*, 2013, **51**, 1647–1655.
- 12 M. Abbaszadeh, D. Krizak and S. Kundu, *Desalination*, DOI:10.1016/j.desal.2019.114116.
- 13 D. F. Ogletree, H. Bluhm, E. D. Hebenstreit and M. Salmeron, *Nucl. Instruments Methods Phys. Res. Sect. A Accel. Spectrometers, Detect. Assoc. Equip.*, 2009, **601**, 151–160.
- 14 M. E. Grass, P. G. Karlsson, F. Aksoy, M. Lundqvist, B. Wannberg, B. S. Mun, Z. Hussain and Z. Liu, *Rev. Sci. Instrum.*, DOI:10.1063/1.3427218.
- 15 P. 1, .
- 16 G. Beamson and D. Briggs, *High Resolution XPS of Organic Polymers: The Scienta ESCA300 Database*, Wiley-VCH, 1992.
- 17 P. 2, .
- 18 J. Russat, *Surf. Interface Anal.*, 1988, **11**, 414–420.
- 19 A. Kruse, C. Thümmeler, A. Killinger, W. Meyer and M. Grunze, *J. Electron Spectros. Relat. Phenomena*, 1992, **60**, 193–209.
- 20 N. Ottosson, E. Wernersson, J. Söderström, W. Pokapanich, S. Kaufmann, S. Svensson, I. Persson, G. Öhrwall and O. Björneholm, *Phys. Chem. Chem. Phys.*, 2011, **13**, 12261.
- 21 N. L. Prisle, N. Ottosson, G. Öhrwall, J. Söderström, M. Dal Maso and O. Björneholm, *Atmos. Chem. Phys.*, 2012, **12**, 12227–12242.
- 22 J. Werner, J. Julin, M. Dalirian, N. L. Prisle, G. Öhrwall, I. Persson, O. Björneholm and I. Riipinen, *Phys. Chem. Chem. Phys.*, 2014, **16**, 21486–21495.
- 23 X. Song, Y. Ma, C. Wang, P. M. Dietrich, W. E. S. Unger and Y. Luo, *J. Phys. Chem. C*, 2012, **116**, 12649–12654.
- 24 T. J. Zimudzi, K. E. Feldman, J. F. Sturmfeld, A. Roy, M. A. Hickner and C. M. Stafford, *Macromolecules*, 2018, **51**, 6623–6629.
- 25 Y. Jin, W. Wang and Z. Su, *J. Memb. Sci.*, 2011, **379**, 121–130.
- 26 L.-T. Lim, I. J. Britt and M. A. Tung, *J. Appl. Polym. Sci.*, 1999, **71**, 197–206.
- 27 R. Puffr and J. Šebenda, *J. Polym. Sci. Part C Polym. Symp.*, 2007, **16**, 79–93.
- 28 Y. Song, F. Xu, M. Wei and Y. Wang, *J. Phys. Chem. B*, 2017, **121**, 1715–1722.
- 29 D. F. Savage, P. F. Egea, Y. Robles-Colmenares, J. D. O. III and R. M. Stroud, *PLoS Biol.*, 2003, **1**, e72.
- 30 L. R. Dartnell, *Astrobiology*, 2011, **11**, 551–582.
- 31 G. Xu and M. R. Chance, *Chem. Rev.*, 2007, **107**, 3514–3543.
- 32 C. Laffon, S. Lacombe, F. Bournel and P. Parent, *J. Chem. Phys.*, 2006, **125**, 204714.
- 33 J. K. Lee, K. L. Walker, H. S. Han, J. Kang, F. B. Prinz, R. M. Waymouth, H. G. Nam and R. N. Zare, *Proc. Natl. Acad. Sci.*, 2019, **116**, 19294–19298.
- 34 T. H. Lay, J. W. Bozzelli and J. H. Seinfeld, *J. Phys. Chem.*, 1996, **100**, 6543–6554.
- 35 X.-M. Pan, M. N. Schuchmann and C. von Sonntag, *J. Chem. Soc. Perkin Trans. 2*, 1993, 289.
- 36 E. R. Mysak, J. D. Smith, P. D. Ashby, J. T. Newberg, K. R. Wilson and H. Bluhm, *Phys. Chem. Chem. Phys.*, 2011, **13**, 7554–7564.